THE JOURNAL OF PHYSICAL CHEMISTRY B

Article

pubs.acs.org/JPCB

Simulation of the Amide I Infrared Spectrum in Photoinduced Peptide Folding/Unfolding Transitions

Laura Zanetti-Polzi,*[,†,‡] Massimiliano Aschi,[†] Andrea Amadei,[¶] and Isabella Daidone*[,†]

[†]Dipartimento di Scienze Fisiche e Chimiche, University of L'Aquila, via Vetoio (Coppito 1), 67010 Coppito (AQ), Italy

[‡]Center S3, Institute of Nanoscience - CNR, Via Campi 213/A, 41125 Modena, Italy

[¶]Dipartimento di Scienze e Tecnologie Chimiche, University of Rome "Tor Vergata", via della Ricerca Scientifica 1, 00133 Rome, Italy

ABSTRACT: The amide I′ infrared spectrum of a α-helical photoswitchable peptide is calculated here by means of a mixed quantum mechanics/molecular dynamics theoretical−computational methodology based on the perturbed matrix method (PMM). The contribution of specific residues to the total spectrum is also analyzed and the results compared to previous experimental spectroscopic data, obtained by means of site-specific isotope labeling at different residues, resulting in good agreement. One of the residues (Ala7) shows atypical spectroscopic behavior in both the experimental and calculated spectra, i.e., the folded-state amide I′ band is shifted to higher frequencies than the unfolded-state one, while the other residues show the opposite behavior. The calculations reveal the origin of this uncommon spectroscopic trend and point to a crucial role of the molecular switch, the presence of which perturbs the conformational sampling of the peptide. Indeed, infrared spectra of the same peptide calculated in the absence of the molecular switch show that the single-residue spectrum of Ala7 does not have any distinguishing feature, resembling the spectra of the other analyzed residues.

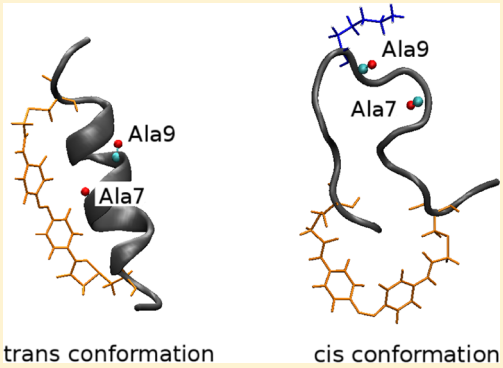

INTRODUCTION

Infrared (IR) spectroscopy can be used to investigate peptide and protein structural properties and folding kinetics.[1,2] Indeed, the amide I band (1700−1600 cm^{-1}), which is due almost entirely to the C═O stretch vibrations of the peptide linkages, is sensitive to the protein secondary structural components. The frequencies of the amide I band are closely correlated to the molecular geometry and hydrogen bonding pattern. Hence, each secondary structure gives rise to a different C═O stretching frequency.[3−7] However, the link of particular frequencies with secondary structures has been made on the basis of semiempirical rules and is often controversial. Moreover, the observed amide I bands are often featureless, due to the extensive overlap of the broad underlying component bands.[8,9] Mathematical data analysis methods can be used to "enhance" the resolution of the protein spectrum,[10−13] but the overlap of secondary structural components remains still significant.

Conventional IR spectroscopy does not probe conformation at the residue level, but, when combined with site-specific isotope labeling, it can be used to obtain local information on the conformation in peptides and proteins. With this approach, individual amide I modes of different residues within a secondary structure can be identified using isotopic substitution. In fact, when a backbone carbonyl is labeled with ^{13}C, the amide I band for that residue is shifted to a lower frequency by 20−40 cm^{-1} and can be resolved from the ^{12}C band, reporting specifically on the conformation of the labeled residues.[14] Even larger shifts (60−70 cm^{-1}) of the amide I band of the labeled residues can be obtained using $^{13}C═^{18}O$ double labeling, allowing a better separation of the signal of the labeled residues from the main band.[15] This widely used technique[14,16−21] provided a large amount of interesting data on different secondary structures. Nevertheless, the structural information obtained often does not have an unequivocal interpretation.

In several recent works,[15,22−31] the inclusion of molecular switches in at-purpose designed peptides has been used to predetermine the conformation of the peptide backbone, thus obtaining IR spectra of easier interpretation, in order to investigate the folding and unfolding kinetics. Indeed, in photoswitchable peptides a cross-linked photoisomerizable moiety drives the transition between the folded and unfolded state. This allows reversible control of the structure and study of both folding and unfolding for one molecule. Azobenzene is widely used as a photoswitch as it determines the helix propensity of the peptide it is linked to: if the azobenzene is in the *trans* state its end-to-end distance roughly matches three helix loops stabilizing the helicity of the peptide. In the *cis* state, on the contrary, the end-to-end distance is too short and the helix is destabilized. In addition, ultrafast kinetics (few ps) of azobenzene are well suited for the design of small, defined

Received: July 8, 2013
Revised: September 17, 2013
Published: September 18, 2013

   dx.doi.org/10.1021/jp406708p | *J. Phys. Chem. B* 2013, 117, 12383−12390

model systems that allow detailed folding studies to be carried out both experimentally and theoretically.[32−36] Such model peptides can indeed bridge the time gap between experimental folding studies and theoretical folding simulations.

Theoretical and computational methods that model protein and peptide IR spectroscopic behavior are thus very useful, when coupled to experimental techniques, to study both folding kinetics and structural properties of these small model systems. Many approaches have been proposed to reproduce the frequency position and line shape of the amide I absorption band.[1,37−50] Among others, a mixed quantum mechanics/molecular dynamics (QM/MD) theoretical-computational methodology based on the Perturbed Matrix Method (PMM)[51−55] was used to calculate the amide I IR spectra of a number of peptides, giving results in good agreement with the experimental ones and aiding in the interpretation of the experimental spectra.[56−59]

In PMM calculations, as in other QM/MM procedures,[60] a portion of the system (the quantum center) is treated at the electronic level, while the rest of the system is described at a classical atomistic level and exerts an electrostatic perturbation on the quantum-center electronic states. Such a perturbative approach allows one to obtain a statistically relevant sampling of the peptide and solvent configurations, which is necessary for a proper calculation of the spectra of complex systems. Moreover, the amide I signal of any residue of the peptide chain may be isolated allowing the comparison with experimental isotope-labeled spectra.[58]

In a recent paper[15] Ihalainen and co-workers studied a photoswitchable α-helical peptide (sequence Ace-AACA-KAAAAKAAACKA-NH_2) at the single amino acid level by employing amide I infrared spectroscopy and $^{13}C{=}{=}^{18}O$ double labeling. The two cysteines of the peptide are linked to an azobenzene moiety that acts as a structural constraint: when the azobenzene is in its *trans* conformation the helix is stabilized while unfolding is induced by the *cis* conformation of the azobenzene (see Figure 1). By means of the single residue analysis they observed an atypical behavior of one residue (Ala7) upon unfolding. The signal of the labeled chromophore shifts indeed to higher frequencies upon folding of the α-helix while the other residues experimentally analyzed show an opposite behavior. The authors of the experimental work hypothesized that the peculiar behavior of Ala7 could depend on the hydrogen bond strengthening upon unfolding at that specific site.

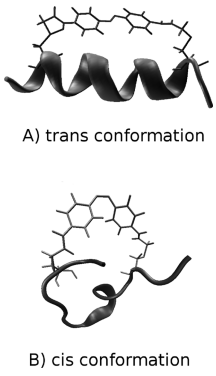

Figure 1. Schematic drawing of the photoswitchable peptide in its *trans* (panel A) and *cis* (panel B) conformations. Note that the *trans* conformation stabilizes the helical structure while the *cis* conformation induces the unfolding of the peptide.

Here the PMM/MD approach is used to calculate the amide I′ (i.e., the amide I in D_2O) spectra of the same peptide studied experimentally.[15] Amide I′ spectra are calculated with the molecular switch both in the *trans* and in the *cis* state, focusing also on the contribution of specific residues to the total spectrum in order to compare the results with the experimental ones.[15] The agreement between the experimental and the calculated spectra is very good and the uncommon behavior of the Ala7 residue is well reproduced and clarified. MD simulations of the same peptide in the absence of the azo-moiety are also performed in order to investigate the role of the molecular switch on the peptide accessible conformational space and on its spectroscopic behavior.

THEORY

The methodology used here to reconstruct amide I′ infrared spectra has been explained in detail in previous articles.[56,61,62] Hereafter, the theoretical basis of PMM calculations and the computational procedure used to obtain vibrational spectra of solvated peptides are briefly outlined.

The PMM/MD approach is based on the combined use of quantum mechanical first principles and an extended phase space sampling as provided by MD simulations. The underlying philosophy of the methodology is to reconstruct the electronic−vibrational quantum states of interest for any given suitable atomistic force field that provides the semi-classical behavior of the system. Hence, the use of empirical parameters is avoided and an extended sampling of the atomic−molecular phase space is maintained.

In PMM calculations,[51−55] similarly to other mixed quantum-classical procedures,[60,63,64] it is essential to predefine a portion of the system to be treated at electronic level, hereafter termed as quantum center (QC), with the rest of the system described at a classical atomistic level exerting the perturbation on the QC electronic states.

The QC used here to model each peptide group along the peptide backbone is trans-N-methylamide (NMA). An orthonormal set of unperturbed electronic Hamiltonian ($\tilde{H}^0$) eigenfunctions (ϕ_j^0) are initially evaluated on the QC structure of interest (see Methods). Then, after having fitted trans-NMA on the given peptide group, the perturbed electronic ground state energy is calculated for each peptide group with the following procedure. Indicating with ν and $\boldsymbol{E}$ the perturbing electric potential and field, respectively, exerted by the environment on the QC (typically obtained by the environment atomic charge distribution and evaluated in the QC center of mass), the perturbed electronic Hamiltonian ($\tilde{H}$) for each QC-environment configuration (as generated by the MD simulation) can be constructed

$$\tilde{H} \simeq \tilde{H}^0 + \tilde{I} q_T \mathcal{V} + \tilde{Z}_1 + \Delta V \tilde{I} \tag{1}$$

$$[\tilde{Z}_1]_{j,j'} = -\boldsymbol{E}\cdot\langle \phi_j^0 | \hat{\mu} | \phi_{j'}^0 \rangle \tag{2}$$

where q_T, $\hat{\boldsymbol{\mu}}$, and ϕ_j^0 are the QC total charge, dipole operator, and unperturbed electronic eigenfunctions, respectively, ΔV approximates all the higher order terms as a simple short-range potential, $\tilde{I}$ is the identity matrix, and the angled brackets indicate integration over the electronic coordinates. The diagonalization of $\tilde{H}$ provides a set of eigenvectors and eigenvalues representing the QC perturbed electronic eigen-

dx.doi.org/10.1021/jp406708p | J. Phys. Chem. B 2013, 117, 12383−12390

states and energies. Note that the side chain of the considered peptide group, the N-1 residues, and the solvent define the perturbing environment at each configuration generated by the MD simulation. Hence, via a polynomial fit of the perturbed electronic ground state energy along the mode coordinate, the perturbed frequencies for each oscillator along the peptide at each MD frame can be obtained.

The basic approximation of the methodology presented so far is that, for typical quantum vibrational degrees of freedom, the environment perturbation does not significantly alter the vibrational modes (i.e., the mass-weighted QC Hessian eigenvectors) but only the related eigenvalues. Such an assumption provides a good approximation when, under the perturbation, a vibrational mode remains largely uncoupled from the other QC modes as well as from the vibrational modes of the solvent molecules. When mode coupling effects due to interacting vibrational centers ought to be considered, excitonic effects must be included in the calculations. The perturbed frequencies for each oscillator, k, are thus used to include the excitonic effect by the construction and diagonalization of the excitonic vibrational Hamiltonian matrix (i.e., the Hamiltonian matrix for the interacting chromophores built by using only the excited vibronic states of interest) given by[62]

$$\tilde{H} = \tilde{I}\mathcal{U}_{vb,0} + \Delta\tilde{H} \tag{3}$$

with $U_{vb,0}$ the (vibronic) ground state energy of the interacting chromophores and $\Delta\tilde{H}$ the excitation matrix providing the excitonic coupling (within the dipolar approximation) among the vibrational excitations for the considered modes of all the chromophores.[62] In the present case we consider only the amide I mode of each residue. By diagonalizing the excitation matrix and using the transition dipole for the $0 \rightarrow i$ excitonic transition ($\boldsymbol{\mu}_{0,i}$) as obtained via the excitonic eigenvectors, we may reconstruct the spectral signal of the excitonic system by summing the absorbance due to each $0 \rightarrow i$ transition, providing

$$\in(\nu) = \sum_i \frac{|\boldsymbol{\mu}_{0,i}|^2 \rho_i(\nu) h\nu}{6 \in_0 c\hbar^2} \tag{4}$$

with ρ_i the probability density in ν frequency space for the ith excitation and $\in_0$ is the vacuum dielectric constant.

METHODS

Unperturbed Quantum Chemical Calculations. The details of the unperturbed quantum chemical calculations are described in previous works[56−59] and are briefly summarized hereafter. As a model of the peptide group, i.e., the quantum center to be explicitly treated at electronic level, trans-NMA was chosen. Quantum chemical calculations were carried out on the isolated trans-NMA molecule at the Time Dependent Density Functional Theory (TDDFT) with the 6-31+G(d) basis set. This level of theory was selected because it represents a good compromise between computational costs and accuracy. The mass-weighted Hessian matrix was calculated on the optimized geometry at the B3LYP/6-31+G(d) level of theory and subsequently diagonalized to obtain the unperturbed eigenvectors and related eigenvalues. The eigenvector corresponding in vacuo to the amide I′ mode was, then, used to generate a grid of points (i.e., configurations) as follows: a step of 0.05 a.u. was adopted and the number of points was set to span an energy range of 20 KJ/mol (in the present case 31 points). For each point, six unperturbed electronic states were then evaluated at the same level of theory providing the basis set for the PMM calculations.

Molecular Dynamics Simulations. A series of 100 ns long MD simulations of the peptide (sequence Ace-AACAKAAAA-KAAACKA-NH_2) in explicit solvent was performed: three MD simulation with the peptide bound to the azobenzene and three MD simulations of the free peptide. In the presence of the molecular switch, one simulation was performed with the azobenzene in the *trans* conformation starting from a helical structure of the peptide and two simulations starting from two unstructured configurations of the peptide with the azobenzene in the *cis* conformation. In the absence of the molecular switch, one MD simulation was started from the same helical configuration mentioned above and two simulations from the two unstructured configurations used in the case of the peptide linked to the azo-moiety. In order to generate the two unstructured configurations, a short simulation of 10 ns was performed starting from an extended configuration and the structures sampled at 9 and 10 ns of the trajectory were selected. The helical and extended starting structures of the peptide were modeled with the program Molden 3.8.[65]

The MD simulations were performed with the GROMACS software package[66] and the OPLS-AA all-atom force field[67] was used for the peptide. The charges of the azobenzene were calculated using RESP[68] with B3LYP/6-31+G* calculations with the package GAMESS (US).[69] Torsion angles were calculated at the same level of theory. The water was modeled using the SPC representation.[70] Each of the starting conformations was placed in a dodecahedral water box large enough to contain the peptide and at least 1.0 nm of solvent on all sides. Periodic boundary conditions were used and the long-range electrostatic interactions were treated with the particle mesh Ewald method.[71] The bond lengths were fixed,[72] and a time step of 2 fs for numerical integration of the equations of motion was used. Simulations were performed in the NVT ensemble with isokinetic temperature coupling[73] keeping the temperature constant at 300 K.

RESULTS AND DISCUSSION

Three MD simulations of the peptide cross-linked by the azo-moiety were performed, one with the azo-moiety in the *trans* conformation and two with the azo-moiety in the *cis* conformation. Analysis of the simulations shows that changing the azobenzene from the *trans* to the *cis* conformation reduces the mean helicity of the peptide from ∼80% to ∼13%. These data are in good agreement with the experimental work[15] that reports a mean helicity of ∼60% in the *trans* state and of ∼15% in the *cis* state.

Amide I′ infrared spectra of the peptide with the azo-moiety in the two different conformations were calculated using the three simulations, with results shown in Figure 2. The calculated spectra reproduce the experimental high-frequency shift upon unfolding, resulting in a positive−negative trend of the folded−unfolded difference spectrum. The frequency shift between the positive and negative peak of the difference spectra is ∼45 cm^{-1} and ∼30−35 cm^{-1} in the calculated and experimental[15] spectra, respectively. The slight discrepancy between the calculated and experimental frequency shift could depend, among other things, on the higher helical content of the peptide observed in the simulation with the azo-moiety in the *trans* conformation with respect to the experimental value (∼80% vs ∼60%).

dx.doi.org/10.1021/jp406708p | J. Phys. Chem. B 2013, 117, 12383−12390

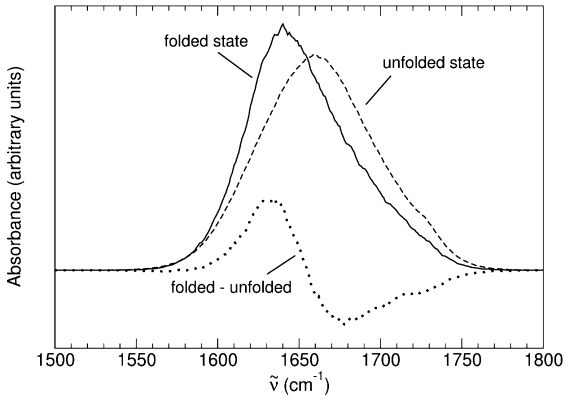

Figure 2. Computed IR spectra in the amide I′ region of the photoswitchable peptide at 300 K. Continuous line: spectrum of the peptide with the azobenzene in the *trans* conformation (folded); dashed line: spectrum of the peptide with the azobenzene in the *cis* conformation (unfolded); dotted line: *trans* state spectrum minus *cis* state spectrum (folded−unfolded). Note that the calculated spectra were shifted to lower frequencies by 65 cm^{-1} in order to align the positive peak of the difference spectrum with the experimental one.[15]

Single-residue spectra were then calculated. The *trans*−*cis* difference spectra of residues Ala7 and Ala9 are reported in Figure 3 together with the corresponding experimental signals

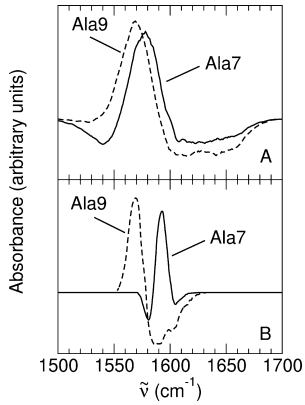

Figure 3. Panel A: Computed single-residue IR difference spectra between the *trans* and *cis* states (*trans*−*cis*) of the photoswitchable peptide at 300 K. Two residues are reported: continuous line, Ala7; dashed line, Ala9. Panel B: Experimental signals of the isotope-labeled Ala7 (continuous line) and Ala9 (dashed line). Note that the calculated spectra were downshifted by 130 cm^{-1} in order to align the positive peak of Ala 9 with the corresponding experimental peak.

obtained by isotope labeling at the corresponding sites.[15] It can be seen from the figure that the *trans*−*cis* difference spectrum of Ala9 shows the positive−negative feature common in folded−unfolded difference spectra, that corresponds to a shift to higher frequencies when the peptide is in its unfolded state. On the contrary, the difference spectrum of Ala7 shows an uncommon behavior, resulting in a *trans*−*cis* difference spectrum with a negative−positive−negative trend. Although the computed and experimental spectra differ (for example, the peaks of the experimental spectra are narrower than the computed ones), the trends of the difference spectra are in qualitative agreement.

The uncommon feature of the *trans*−*cis* difference spectrum of Ala7 has been suggested to arise from a "stronger" hydrogen bonding of the C═O group in the ensemble with the azobenzene in the *cis* conformation than in the ensemble with the azobenzene in the *trans* conformation.[15] In order to test this hypothesis, the hydrogen bonding network of the C═O groups of Ala9 and Ala7 in the MD simulation were thus studied. From the analysis, the mean number of hydrogen bonds (HB) is very similar for the two residues both in the *trans* and in the *cis* state. In fact, the mean number of HB is 0.91 for Ala9 and 0.92 for Ala7 in the *trans* state and 0.91 for Ala9 and 0.94 for Ala7 in the *cis* state. Hence, the uncommon feature of the difference spectrum of Ala7 does not seem to be related, at least in the present case, to a peculiar hydrogen bonding pattern in the *trans* or in the *cis* state.

In one of our previous works[56] the relative frequency positions of the folded and unfolded state single-residue spectra were related, rather than to the local formation of hydrogen bonds, more in general to the exposure of the considered residue to polar atoms. In particular it was found that a decrease in the exposure to polar atoms (of both the protein and the solvent) leads to a shift of the amide I′ band toward higher frequencies. The exposure to polar atoms of the C═O groups of Ala7 and Ala9 was, thus, examined both in the *trans* and in the *cis* states. The radial distribution function of polar atoms around the C═O group of Ala7 at close distances (<0.5 nm) is higher in the *cis* than in the *trans* state (panel A of Figure 4).

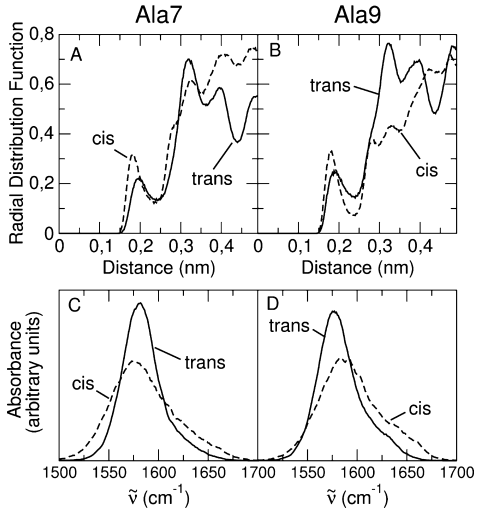

Figure 4. Panels A and B: Radial distribution functions of the polar atoms (of the solvent and of the peptide) around the carbonyl groups of Ala7 (panel A) and Ala9 (panel B) in the *trans* (solid line) and *cis* (dashed line) state. Panels C and D: Single-residue computed IR spectra of Ala7 (panel C) and Ala9 (panel D) in the *trans* (solid line) and *cis* (dashed line) state.

On the contrary, the radial distribution function of polar atoms around the C═O group of Ala9 is lower in the *cis* state than in the *trans* state (panel B of Figure 4). In agreement with our previous work,[56] we find here that a lower exposure to polar atoms leads to a blueshift of the amide I′ frequency. In fact, the peak of the *cis*-state spectrum of Ala9 is at a higher frequency than the peak of the *trans*-state spectrum (panel C of Figure 4), while the opposite is true for the residue Ala7 (panel D of Figure 4), resulting in *trans*−*cis* difference spectra with different trends (see Figure 3A). It is also worth noting that the main difference in the radial distribution functions of the polar atoms around the carbonyl groups of Ala7 and Ala9 arises at distances over 0.25 nm (see panels A and B of Figure 4). Interestingly,

dx.doi.org/10.1021/jp406708p | J. Phys. Chem. B 2013, 117, 12383−12390

this distance threshold matches the characteristic HB distance: the peaks below this distance (around 0.2 nm) are thus likely to represent the polar atoms hydrogen bonded to the C═O groups of Ala7 and Ala9. As can be observed in Figure 4 these peaks are very similar for the two residues, in agreement with the previous observation that the mean number of HB is almost the same for Ala7 and Ala9.

In order to analyze a possible effect of the molecular switch on the atypical spectroscopic behavior of Ala7, simulations of the peptide in the absence of the azobenzene were performed. During the MD simulations of the free peptide both helical and unfolded conformations are sampled, with a mean helicity of ∼40% (the corresponding experimental estimate is ∼35%[74]). The analysis of the trajectories shows that, not surprisingly, the unfolded structures of the free peptide have a considerably higher structural flexibility than the unfolded structures induced by the *cis* conformation of the azobenzene. Indeed, the trace of the covariance matrix of the C_α carbons, related to the chain flexibility, is 1.81 nm^2 in the presence of the azobenzene in the *cis* state and is 4.11 nm^2 in the absence of the molecular switch and when the peptide samples unfolded configurations. This means that the flexibility of the peptide chain in the unfolded state is reduced by 56% in the presence of the azo-moiety. Instead, the two helical ensemble in the presence and absence of the *trans* conformation of the azobenzene show similar structural flexibility. A marked effect of the molecular switch on the chain flexibility was already pointed out by means of MD simulations.[15,36]

Amide I′ spectra of the folded and unfolded state (i.e., the ensemble of structures with some and none helical content, respectively) were calculated (see Figure 5). The unfolded-state

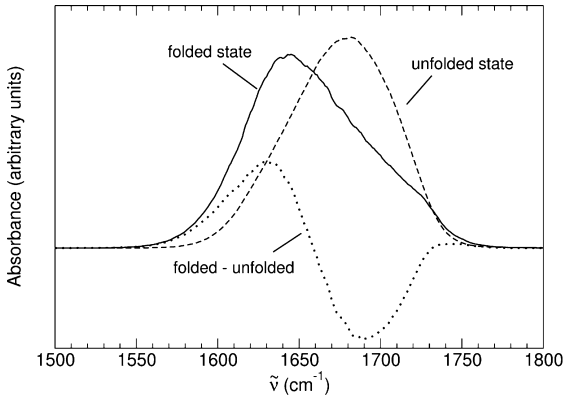

Figure 5. Computed IR spectra in the amide I′ region of the free peptide at 300 K. Continuous line: helical folded state; dashed line: unfolded state; dotted line: folded state spectrum minus unfolded state spectrum. Note that the spectra of the free peptide are shifted to lower frequencies by 65 cm^{-1}, as done for the spectra in the presence of the azo-moiety.

spectrum of the free peptide is shifted to higher frequencies by ∼80 cm^{-1} with respect to the corresponding one in the presence of the molecular switch, while the peaks of the folded-state spectra are almost at the same frequency (see Figure 2 and Figure 5). The huge shift of the unfolded-state peaks is possibly related to the marked differences in structural flexibility described above. No other remarkable differences can be observed between the spectra in the absence and in the presence of the azobenzene.

Single-residue spectra were, then, calculated. In Figure 6 the difference spectra obtained by subtracting the spectrum of the

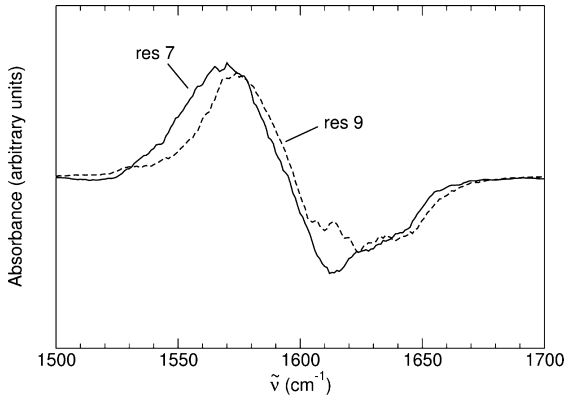

Figure 6. Computed single-residue IR difference spectra between the folded and unfolded state (folded−unfolded) of the free peptide at 300 K. Two residues of the free peptide are reported: continuous line, Ala7; dashed line, Ala9. Note that the spectra are shifted lo lower frequencies by 130 cm^{-1}, as done for the single-residue spectra in the presence of the azo-moiety.

unfolded state from the spectrum of the folded state are reported for Ala7 and Ala9. The data clearly show that in the absence of the azobenzene the two residues share the usual positive−negative trend of the difference spectrum. Coherently, the C═O group exposure to polar atoms is similar for Ala7 and Ala9, i.e., the *cis* state is less exposed than the *trans* state (see Figure 7). Hence, the single-residue spectrum of Ala7 in the free peptide is different from the one obtained in the presence of the azo-moiety (see Figure 3A).

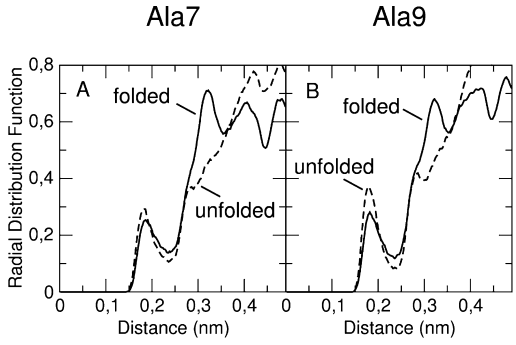

Figure 7. Radial distribution functions of the polar atoms around the carbonyl groups of Ala7 (panel A) and Ala9 (panel B) in the folded (solid line) and unfolded (dashed line) states of the free peptide.

In order to explain at a molecular level the origin of the differences in the exposure of the C═O groups of Ala7 and Ala9 in the presence of the azo-moiety, two representative snapshots of the peptide with the azobenzene in the *trans* and *cis* states are reported in Figure 8. Note that the single unfolded structure of the peptide with the azobenzene in the *cis* state reported in the figure is representative of the whole unfolded ensemble because, as mentioned above, the presence of the azobenzene gives rise to a notable rigidity of the peptide. It can be seen that the C═O group of Ala7 is more exposed to the solvent in the *cis* state, while in the *trans* state it is partially screened from the solvent and the peptide polar atoms by the presence of the azo-moiety, which is mainly hydrophobic. On

dx.doi.org/10.1021/jp406708p | J. Phys. Chem. B 2013, 117, 12383−12390

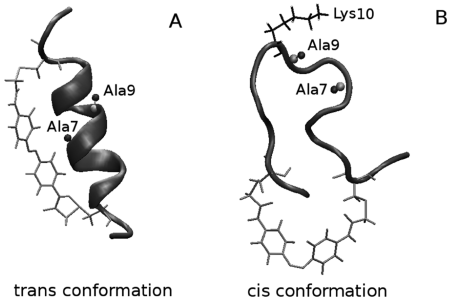

Figure 8. Representative structures of the peptide with the azobenzene in the *trans* (panel A) and *cis* (panel B) state. The carbonyl groups of Ala7 and Ala9 are represented by ball-and-stick models. In the *trans* conformation the C═O group of Ala7 is oriented toward the azobenzene while the C═O group of Ala9 is exposed to the solvent. Note that such a conformation is retained during the whole MD simulation. In the *cis* conformation the side chain of Lys10 is also highlighted with sticks showing its bending toward the C═O group of Ala9.

the contrary, the C═O group of Ala9 is almost fully exposed to the solvent in the *trans* state, while in the *cis* conformation it is partially screened by the aliphatic portion of the side chain of the nearby lysine residue. This last result is in agreement with what was found in our previous work mentioned above,[56] in which a lower exposure to polar atoms in the unfolded state was explained with a screening effect on the C═O group of an hydrophobic side chain (either of the considered residue or of the neighbor residues).

The atypical spectral behavior of Ala7, observed both in the experimental spectra and in the spectra calculated here, has been demonstrated to depend on the presence of the molecular switch experimentally used to induce the folded and unfolded conformations of the peptide. The presence of the azobenzene causes indeed a different exposure to polar atoms of the C═O group of Ala7 with respect to other residues with a common spectral behavior. The exposure to polar atoms results in high correlation to the frequency position of the amide I′ peak and, in this particular case, it seems to be the main interaction driving the spectral behavior, rather than just the presence or absence of hydrogen bonding.

■ CONCLUSIONS

Infrared spectroscopy is widely used to understand the conformation of peptides and proteins in solution (e.g., folded or unfolded state) and to obtain information about their secondary structure. Nevertheless, the interpretation of IR spectra is often non equivocal and theoretical methodologies able to model peptide and protein spectroscopic behavior are very useful to clarify the structural origin of some spectral features.

Here, the infrared spectra of a photoswitchable peptide were calculated both in the *trans* and in the *cis* state of the azobenzene moiety used as molecular switch (corresponding respectively to a higher and lower helicity of the peptide) and compared to the experimental ones obtaining a good agreement. Moreover, single-residue spectra were calculated and compared to the experimental spectra obtained by the isotope-labeling at the corresponding sites showing a good agreement. In particular, the peculiar, experimentally observed, trend of the *trans*−*cis* difference spectrum of Ala7 was observed also in the calculated spectrum, confirming the reliability of the PMM approach in modeling the IR spectra.

The uncommon behavior of Ala7 was explained by analyzing the exposure to polar atoms of the C═O group of the different residues in the *trans* and in the *cis* state. Indeed, unlike the other residues, the exposure of the C═O of Ala7 to polar atoms is higher in the *cis* than in the *trans* state, leading to the uncommon spectral behavior experimentally observed. This feature has been demonstrated to depend on the presence of the azobenzene: the calculated single-residue difference spectrum of Ala7 in the absence of the azo-moiety does not show the uncommon behavior mentioned above. The different exposure to polar atoms can be thus ascribed to the presence of the azobenzene both in the *trans* and in the *cis* state. In the *trans* state the azo-moiety exerts a direct effect on the exposure to polar atoms of the C═O group of Ala7, screening it from the surrounding environment. In the *cis* state the azobenzene has an indirect effect: the C═O group of Ala7 is blocked in a position highly exposed to polar atoms as a consequence of the low flexibility of the peptide chain which is due to the presence of the molecular switch. Indeed, the effect of the azobenzene on the overall conformation of the peptide was analyzed, showing that it considerably limits the number of the peptides unfolded conformations.

Molecular switches are widely used in folding and unfolding studies of at-purpose designed peptides. However, as already suggested,[15,36] the present work confirms that such peptides can not always be used as model systems for real secondary structures, as the molecular switch can considerably influence important structural and dynamical properties. The analysis of the present calculated spectra elucidates the influence of the azo-moiety in the resulting spectral signal. Moreover, by clarifying the origin of the peculiar features of the spectra of the peptide analyzed here, it emerges that analyzing only the hydrogen bonding network gives an incomplete picture. In fact, the more general exposure to polar atoms in the folded and unfolded state seems to have a determining effect on the frequency position of the corresponding spectra.

■ AUTHOR INFORMATION

Corresponding Author

*E-mail: laura.zanettipolzi@nano.cnr.it; isabella.daidone@univaq.it.

Notes

The authors declare no competing financial interest.

■ ACKNOWLEDGMENTS

The authors acknowledge Michele Salvi and Giuseppe Guarracino for their contribution to the MD simulations. The authors acknowledge CINECA Italy for the project ISCRAC IsC08_ETBIO.

■ REFERENCES

(1) Krimm, S.; Bandekar, J. Vibrational Spectroscopy and Conformation of Peptides, Polypeptides and Proteins. *Adv. Protein Chem.* **1986**, *38*, 181−364.

(2) Surewicz, W.; Mantsch, H. New Insight into Protein Secondary Structure from Resolution-Enhanced Infrared Spectra. *Biochim. Biophys. Acta* **1988**, *952*, 115−130.

(3) Dong, A.; Huang, P.; Caughey, W. Protein Secondary Structure in Water from Second-Derivative Amide I Infrared Spectra. *Biochemistry* **1990**, *29*, 3303−3308.

(4) Venyaminov, S.; Kalnin, N. Quantitative IR Spectrophotometry of Peptide Compounds in Water (H_2O) Solution. II. Amide

Absorption Bands of Polypeptide and Fibrous Protein in α-, β-, and Random Coil Conformation. *Biopolymers* **1990**, *30*, 1259−1271.
(5) Surewicz, W. K.; Mantsch, J. H. H.; Chapman, D. Determination of Protein Secondary Structure by Fourier Transform Infrared Spectroscopy: A Critical Assessment. *Biochemistry* **1993**, *32*, 389−394.
(6) Kumosinski, T. F.; Unruh, J. J. Quantitation of the Global Secondary Structure of Globular proteins by FTIR Spectroscopy: Comparison with X-ray Crystallographic Structure. *Talanta* **1996**, *43*, 199−219.
(7) Barth, A. Infrared Spectroscopy of Proteins. *Biochim. Biophys. Acta* **2007**, *1767*, 1073−1101.
(8) DeFlores, L. P.; Ganim, Z.; Nicodemus, R. A.; Tokmakoff, A. Amide I′-II′ 2D IR Spectroscopy Provides Enhanced Protein Secondary Structural Sensitivity. *J. Am. Chem. Soc.* **2009**, *131*, 3385−3391.
(9) Kong, J.; Yu, S. Fourier Transform Infrared Spectroscopic Analysis of Protein Secondary Structures. *Acta Biochim. Biophys. Sinica* **2007**, *39* (8), 549−559.
(10) Kauppinen, J.; Moffatt, D.; Mantsch, H.; Cameron, D. A Method for Resolving Intrinsically Overlapped Bands. *Appl. Spectrosc.* **1986**, *35*, 271−276.
(11) Byler, D.; Susi, H. Examination of the Secondary Structure of Proteins by Deconvolved FTIR Spectra. *Biopolymers* **1986**, *25*, 469−487.
(12) Lee, D.; Haris, P.; Chapman, D.; Mitchell, R. Determination of Protein Secondary Structure Using Factor Analysis of Infrared Spectra. *Biochemistry* **1990**, *29*, 9185−9193.
(13) Sarver, R.; Krueger, W. Protein Secondary Structure from Fourier Transform Infrared Spectroscopy: a Data Base Analysis. *Anal. Biochem.* **1991**, *194*, 89−100.
(14) Decatur, S. IR Spectroscopy of Isotope-Labeled Helical Peptides: Probing the Effect of N-acetylation on Helix Stability. *Biopolymers* **2000**, *54*, 180−185.
(15) Ihalainen, J.; Paoli, B.; Muff, S.; Backus, E.; Bredenbeck, J.; Caflisch, G. W. A.; Hamm, P. α-Helix Folding in the Presence of Structural Constraints. *Proc. Natl. Acad. Sci. U.S.A.* **2008**, *105* (28), 9588−9593.
(16) Ludlam, C.; Arkin, I.; Liu, X.; Rothman, M.; Rath, P.; Aimoto, S.; Smith, S.; Engelman, D.; Rothschild, K. Fourier Transform Infrared Spectroscopy and Site-Directed Isotopelabeling as a Probe of Local Secondary Structure in the Transmembrane Domain of Phospholamban. *Biophys. J.* **1996**, *70* (4), 1728−1736.
(17) Decatur, S.; Antonic, J. Isotope-edited Infrared Spectroscopy of Helical Peptides. *J. Am. Chem. Soc.* **1999**, *121*, 11914−11915.
(18) Brauner, J.; Dugan, C.; Mendelsohn, R. ^{13}C Isotope Labeling of Hydrophobic Peptides. Origin of the Anomalous Intensity Distribution in the Infrared Amide I Spectral Region of β-Sheet Structures. *J. Am. Chem. Soc.* **2000**, *122* (4), 677−683.
(19) Huang, R.; Kubelka, J.; Barber-Armstrong, W.; Silva, R.; Decatur, S.; Keiderling, T. Nature of Vibrational Coupling in Helical Peptides:? an Isotopic Labeling Study. *J. Am. Chem. Soc.* **2004**, *126* (8), 2346−2354.
(20) Hiramatsu, H.; Kitagawa, T. FT-IR Approaches on Amyloid Fibril Structure. *Biochim. Biophys. Acta* **2005**, *1753* (1), 100−107.
(21) Decatur, S. Elucidation of Residue-Level Structure and Dynamics of Polypeptides via Isotope-Edited Infrared Spectroscopy. *Acc. Chem. Res.* **2006**, *39* (3), 169−175.
(22) Kumita, J.; Smart, O.; Woolley, G. Photo-Control of Helix Content in a Short Peptide. *Proc. Natl. Acad. Sci. U.S.A.* **2000**, *97* (8), 3803−3808.
(23) Bredenbeck, J.; Helbing, J.; Behrendt, R.; Renner, C.; Moroder, L.; Wachtveitl, J.; Hamm, P. Transient 2D-IR Spectroscopy:? Snapshots of the Nonequilibrium Ensemble during the Picosecond Conformational Transition of a Small Peptide. *J. Phys. Chem. B* **2003**, *107* (33), 8654−8660.
(24) Wachtveitl, J.; Sporlein, S.; Satzger, H.; Fonrobert, B.; Renner, C.; Behrendt, R.; Oesterhelt, D.; Moroder, L.; Zinth, W. Ultrafast Conformational Dynamics in Cyclic Azobenzene Peptides of Increased Flexibility. *Biophys. J.* **2004**, *86* (4), 2350−2362.
(25) Bredenbeck, J.; Helbing, J.; Kumita, J.; Woolley, G.; Hamm, P. α-Helix Formation in a Photoswitchable Peptide Tracked from Picoseconds to Microseconds by Time-Resolved IR Spectroscopy. *Proc. Natl. Acad. Sci. U.S.A.* **2005**, *102*, 2379−2384.
(26) Aemissegger, A.; Krautler, V.; van Gunsteren, W.; Hilver, D. A Photoinducible β-Hairpin. *J. Am. Chem. Soc.* **2005**, *127* (9), 2929−2936.
(27) Dong, S.; Loweneck, M.; Schrader, T.; Schreier, W.; Zinth, W.; Moroder, L.; Renner, C. A Photocontrolled β-Hairpin Peptide. *Chem.—Eur. J.* **2006**, *12* (4), 1114−1120.
(28) Kolano, C.; Helbing, J.; Kozinski, M.; Sander, W.; Hamm, P. Watching Hydrogen-Bond Dynamics in a β-Turn by Transient two-Dimensional Infrared Spectroscopy. *Nature* **2006**, *444*, 469−472.
(29) Ihalainen, J. A.; Bredenbeck, J.; Pfister, R.; Helbing, J.; Chi, L.; van Stokkum, I. H.; Woolley, G. A.; Hamm, P. Folding and Unfolding of a Photoswitchable Peptide from Picoseconds to Microseconds. *Proc. Natl. Acad. Sci. U.S.A.* **2007**, *104*, 5383−5388.
(30) Hamm, P.; Helbing, J.; Bredenbeck, J. Two-Dimensional Infrared Spectroscopy of Photoswitchable Peptides. *Annu. Rev. Phys. Chem.* **2008**, *59*, 291−317.
(31) Backus, E.; Bloem, R.; Donaldson, P.; Ihalainen, J.; Pfister, R.; Paoli, B.; Caflisch, A.; Hamm, P. 2D-IR Study of a Photoswitchable Isotope-Labeled α-Helix. *J. Phys. Chem. B* **2010**, *114* (10), 3735−3740.
(32) Sporlein, S.; Carstens, H.; Satzger, H.; Renner, C.; Behrendt, R.; Moroder, L.; Tavan, P.; Zinth, W.; Wachtveitl, J. Ultrafast Spectroscopy Reveals Subnanosecond Peptide Conformational Dynamics and Validates Molecular Dynamics Simulation. *Proc. Natl. Acad. Sci. U.S.A.* **2002**, *99*, 7998−8002.
(33) Carstens, H.; Renner, C.; Milbradt, A.; P. Tavan, L. M. Multiple Loop Conformations of Peptides Predicted by Molecular Dynamics Simulations Are Compatible with Nuclear Magnetic Resonance. *Biochemistry* **2005**, *44* (12), 4829−4840.
(34) Nguyen, P.; Gorbunov, R.; Stock, G. Photoinduced Conformational Dynamics of a Photoswitchable Peptide: A Nonequilibrium Molecular Dynamics Simulation Study. *Biophys. J.* **2006**, *91* (4), 1224−1234.
(35) Nguyen, P.; Stock, G. Nonequilibrium Molecular Dynamics Simulation of a Photoswitchable Peptide. *Chem. Phys.* **2006**, *323*, 36−44.
(36) Paoli, B.; Pellarin, R.; Caflisch, A. Slow Folding of Cross-Linked a-Helical Peptides Due to Steric Hindrance. *J. Phys. Chem. B* **2010**, *114*, 2023−2027.
(37) Torii, H.; Tasumi, M. Model Calculations on the Amide I Infrared Bands of Globular Proteins. *J. Chem. Phys.* **1992**, *96*, 3379−3387.
(38) Lee, S. H.; Krimm, S. Ab Initio-Based Vibrational Analysis of α-Poly(L-alanine). *Biopolymers* **1998**, *46*, 283−317.
(39) Kwac, K.; Cho, M. Molecular Dynamics Simulation Study of N-Methylacetamide in Water. I. Amide I Mode Frequency Fluctuation. *J. Chem. Phys.* **2003**, *119*, 2247−2255.
(40) Moran, A.; Mukamel, S. The Origin of Vibrational Mode Couplings in Various Secondary Structural Motifs of Polypeptides. *Proc. Natl. Acad. Sci. U.S.A.* **2004**, *101*, 506−510.
(41) Schmidt, J. R.; Corcelli, S. A.; Skinner, J. L. Ultrafast Vibrational Spectroscopy of Water and Aqueous N-Methylacetamide: Comparison of Different Electronic Structure/Molecular Dynamics Approaches. *J. Chem. Phys.* **2004**, *121*, 8887−8896.
(42) Brauner, J. W.; Flach, C. R.; Mendelsohn, R. A Quantitative Reconstruction of the Amide I Contour in the IR Spectra of Globular Proteins: From Structure to Spectrum. *J. Am. Chem. Soc.* **2005**, *127*, 100−109.
(43) Yang, S.; Cho, M. IR Spectra of N-Methylacetamide in Water Predicted by Combined Quantum Mechanical/Molecular Mechanical Molecular Dynamics Simulations. *J. Chem. Phys.* **2005**, *123*, 134503−134505.
(44) Bour, P.; Keiderling, T. A. Vibrational Spectral Simulation for Peptides of Mixed Secondary Structure: Method Comparisons with the Trpzip Model Hairpin. *J. Phys. Chem. B* **2005**, *109*, 23687−23697.

(45) Gaigeot, M. P.; Vuilleumier, R.; Sprik, M.; Borgis, D. Infrared Spectroscopy of N-Methylacetamide Revisited by ab Initio Molecular Dynamics Simulations. *J. Chem. Theory Comput.* **2005**, *1*, 772−789.
(46) Smith, A. E.; Tokmakoff, A. Amide I two-Dimensional Infrared Spectroscopy of β-Hairpin Peptides. *J. Chem. Phys.* **2007**, *126*, 45108−45111.
(47) Gorbunov, R. D.; Nguyen, P. H.; Kobus, M.; Stock, G. Quantum-Classical Description of the Amide I Vibrational Spectrum of Trialanine. *J. Chem. Phys.* **2007**, *126*, 054509−054518.
(48) Ham, S.; Cha, S.; Choi, J. H.; Cho, M. Amide I Modes of Tripeptides: Hessian Matrix Reconstruction and Isotope Effects. *J. Chem. Phys.* **2003**, *119*, 1451−1461.
(49) Hahn, S.; Ham, S.; Cho, M. Simulation Studies of Amide I IR Absorption and Two-Dimensional IR Spectra of β Hairpins in Liquid Water. *J. Phys. Chem. B* **2005**, *109*, 11789−11801.
(50) Choi, J. H.; Lee, H.; Lee, K. K.; Hahn, S.; Cho, M. Computational Spectroscopy of Ubiquitin: Comparison between Theory and Experiments. *J. Chem. Phys.* **2007**, *126*, 045102−045115.
(51) Aschi, M.; Spezia, R.; Di Nola, A.; Amadei, A. A First Priciples Method to Model Perturbed Electronic Wavefunctions: the Effect of an External Electric Field. *Chem. Phys. Lett.* **2001**, *344*, 374−380.
(52) Spezia, R.; Aschi, M.; Di Nola, A.; Amadei, A. Extension of the Perturbed Matrix Method: Application to a Water Molecule. *Chem. Phys. Lett.* **2002**, *365*, 450−456.
(53) Amadei, A.; D'Abramo, M.; Zazza, C.; Aschi, M. Electronic Properties of Formaldehyde: a Theoretical Study. *Chem. Phys. Lett.* **2003**, *381*, 187−193.
(54) Amadei, A.; Marinelli, F.; D'Abramo, M.; D'Alessandro, M.; Anselmi, M.; Di Nola, A.; Aschi, M. Theoretical Modeling of Vibro-Electronic Quantum States in Complex Molecular Systems: Solvated Carbon Monoxide, a Test Case. *J. Chem. Phys.* **2005**, *122*, 124506−124515.
(55) Amadei, A.; D'Alessandro, M.; D'Abramo, M.; Aschi, M. Theoretical Characterization of Electronic States in Interacting Chemical Systems. *J. Chem. Phys.* **2009**, *130*, 08410−08415.
(56) Daidone, I.; Aschi, M.; Zanetti-Polzi, L.; Nola, A. D.; Amadei, A. On the Origin of IR Spectral Changes upon Protein Folding. *Chem. Phys. Lett.* **2010**, *488*, 213−218.
(57) Zanetti-Polzi, L.; Daidone, I.; Anselmi, M.; Carchini, G.; Di Nola, A.; Amadei, A. Analysis of Infrared Spectra of ß-Hairpin Peptides as Derived from Molecular Dynamics Simulations. *J. Phys. Chem. B* **2011**, *115* (41), 11872−11878.
(58) Zanetti-Polzi, L.; Amadei, A.; Aschi, M.; Daidone, I. Insight into the IR-Spectra/Structure Relationship in Amyloid Fibrils: a Theoretical Study on a Prion Peptide. *J. Am. Chem. Soc.* **2011**, *133* (30), 11414−11417.
(59) Zanetti-Polzi, L.; Daidone, I.; Amadei, A. A Theoretical Reappraisal of Polylysine in the Investigation of Secondary Structure Sensitivity of Infrared Spectra. *J. Phys. Chem. B* **2012**, *116* (10), 3353−3360.
(60) Gao, J.; Truhlar, D. G. Quantum Mechanical Methods for Enzyme Kinetics. *Annu. Rev. Phys. Chem.* **2002**, *53*, 467−505.
(61) Amadei, A.; Daidone, I.; Di Nola, A.; Aschi, M. Theoretical-Computational Modelling of Infrared Spectra in Peptides and Proteins: a new Frontier for Combined Theoretical-Experimental Investigations. *Curr. Opin. Struct. Biol.* **2010**, *20*, 155−161.
(62) Amadei, A.; Daidone, I.; Zanetti-Polzi, L.; Aschi, M. Modeling Quantum Vibrational Excitations in Condensed-Phase Molecular Systems. *Theor. Chem. Acc.* **2011**, *129*, 31−43.
(63) Vreven, T.; Morokuma, K. Chapter 3 Hybrid Methods: ONIOM(QM:MM) and QM/MM. *Annu. Rep. Comp. Chem.* **2006**, *2*, 35−51.
(64) Senn, H. M.; Thiel, W. QM/MM Studies of Enzymes. *Curr. Opin. Chem. Biol.* **2007**, *11*, 182−187.
(65) Schaftenaar, G.; Noordik, J. Molden: a pre- and post-Processing Program for Molecular and Electronic Structures. *J. Comput.-Aided Mol. Des.* **2000**, *14*, 123−134.
(66) Berendsen, H. J. C.; van der Spoel, D.; van Drunen, R. GROMACS: A Message-Passing Parallel Molecular Dynamics Implementation. *Comput. Phys. Commun.* **1995**, *91*, 43−56.
(67) Jorgensen, W.; Tirado-Rives, J. The OPLS [Optimized Potentials for Liquid Simulations] Potential Functions for Proteins, Energy Minimizations for Crystals of Cyclic Peptides and Crambin. *J. Am. Chem. Soc.* **1988**, *110* (6), 1657−1666.
(68) Bayly, C.; Cieplak, P.; Cornell, W.; Kollman, P. A Well-Behaved Electrostatic Potential Based Method Using Charge Restraints for Deriving Atomic Charges: the RESP Model. *J. Phys. Chem.* **1993**, *97*, 10269−10280.
(69) Schmidt, M.; Baldridge, K.; Boatz, J.; Elbert, S.; Gordon, M.; Jensen, J.; Koseki, S.; Matsunaga, N.; Nguyen, K.; Su, S.; Windus, T.; Dupuis, M.; Montgomery, J. General Atomic and Molecular Electronic Structure System. *J. Comput. Chem.* **1993**, *14*, 1347−1363.
(70) Berendsen, H. J. C.; Grigera, J. R.; Straatsma, T. P. The Missing Term in Effective Pair Potentials. *J. Phys. Chem.* **1987**, *91*, 6269−6271.
(71) Darden, T.; York, D.; Pedersen, L. Particle mesh Ewald: An N-log(N) Method for Ewald Sums in Large Systems. *J. Chem. Phys.* **1993**, *98*, 10089−10092.
(72) Hess, B.; Bekker, H.; Berendsen, H. J. C.; Fraaije, J. LINCS: A Linear Constraint Solver for Molecular Simulations. *J. Comput. Chem.* **1997**, *18*, 1463−1472.
(73) Brown, D.; Clarke, J. A Comparison of Constant Energy, Constant Temperature and Constant Pressure Ensembles in Molecular Dynamics Simulations of Atomic Liquids. *Mol. Phys.* **1984**, *51*, 1243−1252.
(74) Marquesee, S.; Robbins, V.; Baldwin, R. Unusually Stable Helix Formation in Short Alanine-Based Peptides. *Proc. Natl. Acad. Sci. U.S.A.* **1989**, *86*, 5286−5290.